International Journal of Pattern Recognition and Artificial Intelligence
Vol. 15, No. 6 (2001) 905–919

CIRCULAR CODED TARGET FOR AUTOMATION OF OPTICAL 3D-MEASUREMENT AND CAMERA CALIBRATION

SUNG JOON AHN and WOLFGANG RAUH
Fraunhofer Institute for Manufacturing Engineering and Automation (IPA), Nobelstr. 12, 70569 Stuttgart, Germany
E-mail: {sja; wor}@ipa.fhg.de

SUNG IL KIM
Sport and Mechanics Laboratory, Korea University, Anam-dong, Sungbuk-gu, 136-701 Seoul, South Korea
E-mail: sun_kim@mail.korea.ac.kr

One of the primary, but tedious, tasks for the user and developer of an optical 3D-measurement system is to find the homologous image points in multiple images, a task that is frequently referred to as the correspondence problem. Along with the solution, error-free correspondence and accurate measurement of image points are of great importance, on which the qualitative results of succeeding camera calibration and 3D-measurements are immediately dependent. In fact, the automation of measurement processes is getting more important with progresses in production, and hence, is of increasing topical interest. In this paper, we present a circular coded target for automatic image point measurement and identification. The applied image processing method will be described in detail, and we will show some application examples of the circular coded target to optical 3D-measurement techniques.

Keywords: Measurement automation; correspondence problem; coded target; form factor; camera calibration; optical 3D-measurement.

1. Introduction

At the moment, basic software and hardware components that are capable of constructing an optical 3D-measuring system are available on the market, providing numerous combinations of measurement principles and methods, thus making the construction of a special or general purpose measuring system possible. Along with software and hardware components, any point target for 3D-measurement is also considered as a part of the measurement system, because the overall measuring performance and the resulting accuracy levels are directly linked to the quality of the image point determination. In addition, a high-level automation of the measuring process, especially of the image point determination and identification, is desirable for the industrial application of optical 3D-measurement techniques.[10]

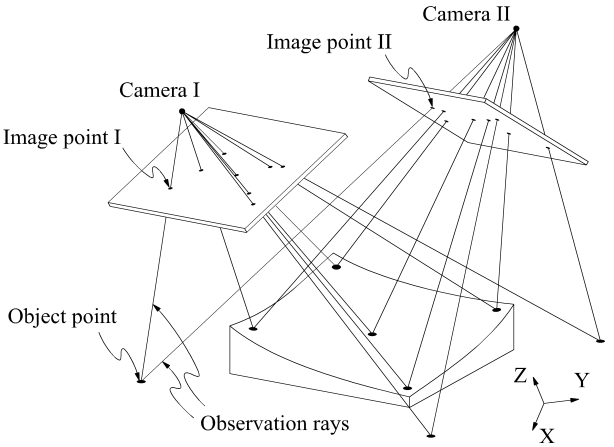

Fig. 1. Typical setup for 3D-point measurement and camera calibration by stereo vision.

In order to make the aim of this paper clear, we consider 3D-point measurement (3D-triangulation) by stereo imaging, in which we like to determine the 3D-coordinates of the object points from the given two images (Fig. 1). A 3D-point is the intersection of the two observation rays drawn from the camera projection centers through the homologous image points of the object point. Thus, for the purpose of 3D-triangulation we need the camera parameters of the two images and the homologous image points of the object point. The homologous image points are to be acquired with the method of image processing, and the camera parameters are to be determined through an analysis of the coordinates of the homologous image points of some object points (camera calibration). Our paper is aimed at the acquisition of the homologous image points (i.e. solving the correspondence problem) using the coded targets detected and identified in the images without orientation information. Of course, if the image orientations are *a priori* known (e.g. through camera calibration), the correspondence problem can be solved by using epipolar constraints. However, in many applications, the image orientations are unknown and must be determined through a camera calibration. Really, determining the image points, and solving the correspondence problem, are the main time-consuming tasks of 3D-measurement and camera calibration for a measurement project with a large number of images taken with unknown camera parameters. Provided that the correspondence problem is solved, the rest of the procedures for camera calibration and 3D-point determination can be automatically carried out.

In recent years, the demand for a coded target guaranteeing automatic, error-free correspondence and accurate image point measurement, has been dramatically increased.[8–12,14,19,21,22] Until now, some coded targets have been accepted more or less for the automation of optical 3D-measurement (Fig. 2).[8,9,11,12,14,17,19–22] Except for the first two, the coded targets in Fig. 2 were developed for the purpose

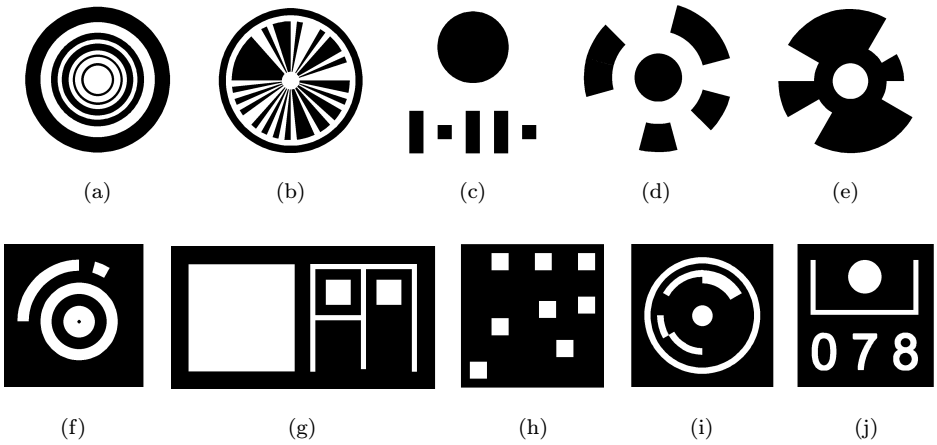

Fig. 2. Various types of coded targets: (a) Russo, 1972; (b) Trenkler, 1981; (c) Wong, 1988; (d) Schneider, 1991; (e) Knobloch, 1992; (f) van den Heuvel, 1992; (g) Homainejad, 1995; (h) Fraser, 1997; (i) Niederöst, 1997, (j) Caesar, 1997.

of automating 3D-measurement procedures. The coding information is embedded in the form of linear, radial or angular bar codes, being decoded by an analysis of the changes of the image gray values along an appropriate image sampling path [Figs. 2(a)–2(f), 2(i)]. Some other coded targets have their coding information in the form of dot code [Fig. 2(h)] or numeric characters [Fig. 2(j)]. All of these coded targets have narrow or cornering geometric features. If the quality or the resolution of the target image is low, or if the lighting condition is unfavorable (e.g. through the projection of a random pattern), the coding information gets destroyed as long as it is being obtained from the change of the image gray values, and an error-free decoding of the coded target will be difficult.

To realize fully automatic 3D-measurement procedures, and accurate image point measurements, we have developed a new circular coded target having only circular elements and circular arrangements (Fig. 3).[2] A circular disc will always be imaged as an ellipse under central projection, and in comparison with other geometric form elements, it is robust against image degrading processes (e.g. defocusing, or changing of the imaging distance and angle). The size and form of the circular coding elements are especially compact, making the overall size of the circular coded target as small as possible. The coding information is to be obtained through an analysis of the positions of the coding elements around the central point mark in binary image, thus, it remains relatively undisturbed by an image degrading process, compared with the coded targets in Fig. 2, whose coding information is to be obtained through an analysis of the image gray value changes along a given sampling path. Because all of the geometric elements and arrangements are circular, the circular coded target is well distinguishable in a natural scene, and only a few simple image processing algorithms (e.g. binarization, form factor analysis and ellipse fitting) are to be applied. We have found great acceptance from the industry,

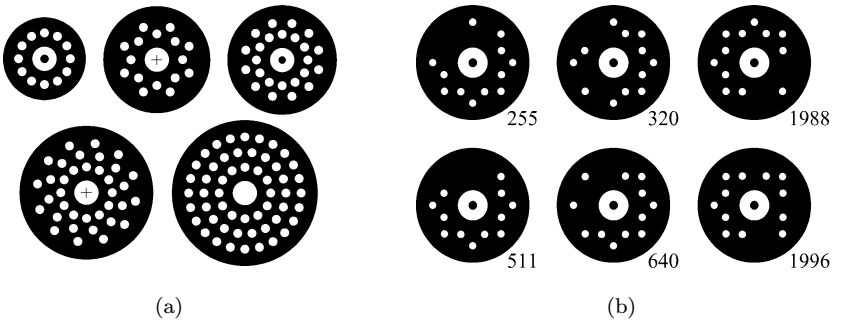

Fig. 3. The proposed circular coded target: (a) Examples of the circular coded target with 12-, 16-, 24-, 36- and 54-bit code lengths; (b) Coding examples of the 16-bit circular coded target with 12 turned on coding points and 2 coding layers. The bit position 0 (upper center) is the parity bit, and 2, 6, 10 and 12 (clockwise) are always turned on.

even in the toughest application of the circular coded target with a superimposed random pattern.[4,13,15] In the current paper, we intend to describe the geometric construction of the target, its image processing and its application to the optical 3D-measurement method.

2. Geometric Construction of the Circular Coded Target

Out of consideration for robust and reliable image processing, the target is geometrically constructed only of circular elements (i.e. circular point mark, circular coding points, and circular background plate (Fig. 3)). The superiority of the circular object target over other geometric features, for the purpose of image point measurement, is also reported in the literature.[7] The identification number of the target is coded down into the circular arrangement of the coding points around the point mark. Additionally, the size and arrangements of the coding points around the point mark are also geometrically prescribed [Figs. 4(b)–4(e)]. We have fully utilized all these geometric absolute/relative constraints on the target construction with image processing, and have achieved very robust and reliable image point measurements and identifications. If the size of the point mark becomes a matter of 3D-measurement accuracy, because of the *eccentricity errors* resulting from the central projective imaging of the circular object, we select the appropriate diameter of the point mark, guaranteeing reliable and accurate image point determination.[5] Instead of the point mark, we can also treat the background plate, or the additional centering mark in the middle of the point mark, as the measuring object. As a result, a wide range of imaging distances will be allowed.

3. Image Processing for the Circular Coded Target

To minimize the necessary computing costs, binary image processing is preferably applied here, except for the subpixel accurate edge detection of the contour points of

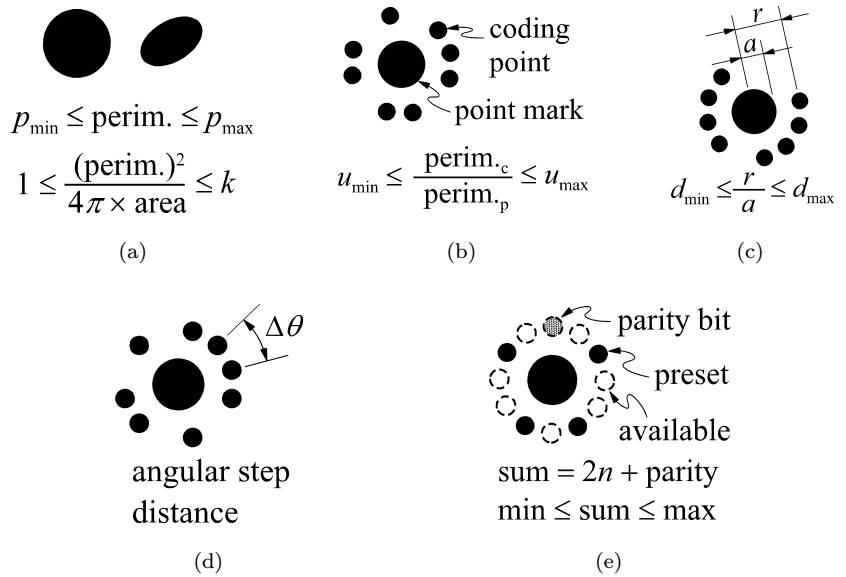

Fig. 4. Geometric features of the circular coded target: (a) Size and form factor of the image of a circular disc; (b) Normalized size of the coding points against the point mark; (c) Normalized distance of the coding points from the center of the point mark; (d) Angular step distance of the coding points; (e) Total sum and preset pattern of the bit positions including the parity bit.

the point mark. From the gray image we can accurately determine the image point of the point mark, and from the binary image we reliably extract the code information. First, we know from the given imaging conditions the approximate size of the image ellipse of the used point mark [Fig. 4(a)], assuming that an image ellipse is the projection of an object circle onto the image plane. In addition, such an image ellipse is a relatively compact image feature for a natural scene, where the compactness can be represented by the *form factor* as below:

$$\text{Form factor} = \frac{(\text{perimeter})^2}{4\pi \times \text{area}}\,. \tag{1}$$

The form factor has a minimum value of 1 by a circular disc, and is greater than 1 for all other geometric features. For an ellipse, the image of an object circle, the form factor increases with the imaging angle monotonously and moderately up to 1.5 at the angle of 70° [Figs. 5(a) and 5(b)]. We have also investigated the effect of the contour discretization onto the form factor of a circular image object [Figs. 5(c) and 5(d)]. Here, we assumed that the discretized contour of a circular image object could be approximately represented as a regular polygon. We conclude that the effect of discretization will be negligible if the size of an image object is larger than 5 pixel in diameter.

If we were to put bounds to the size and form factor of an image object according to the results in Fig. 5, we can detect all point mark candidates in the image plane [Fig. 4(a)] whose validity will be individually qualified in the subsequent

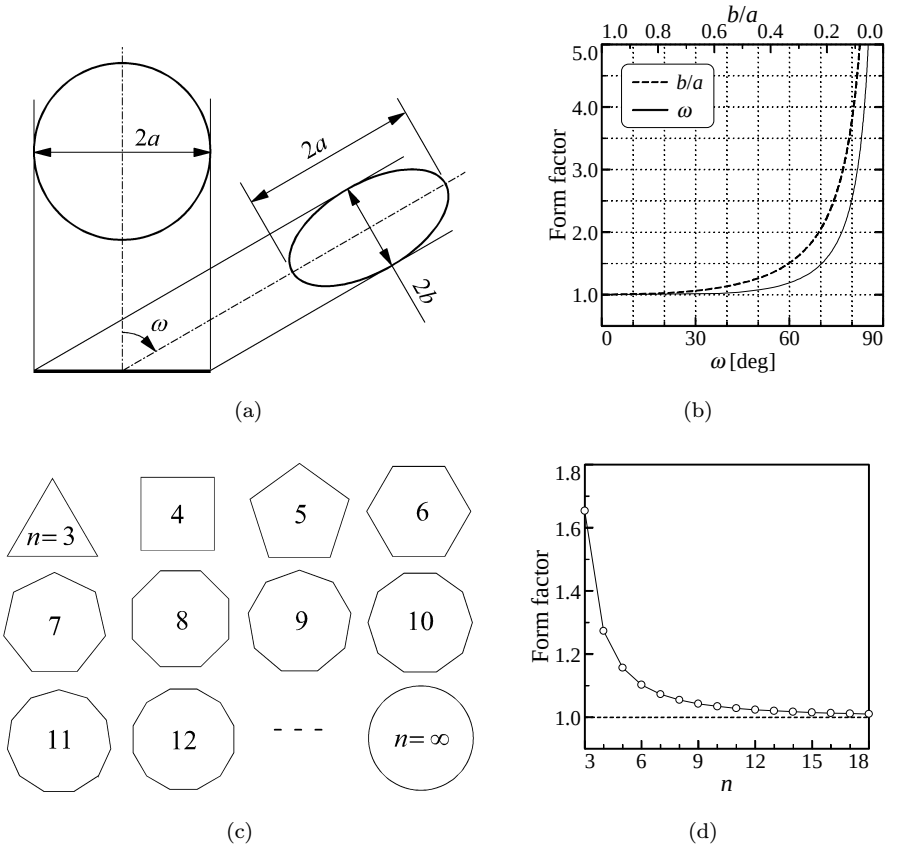

Fig. 5. Form factor of an image object: (a) Ellipse as the image of an object circle assuming a parallel projection; (b) Dependence of the form factor on the projection angle; (c) Regular polygons as the approximation of the contour of a circular image object; (d) Form factor of regular polygons.

processing steps. Next, around a point mark candidate, we search for smaller image objects as the coding points of the point mark satisfying the membership criteria [Figs. 4(b) and 4(c)]. After a proper coordinate transformation, with an inverse affine transformation, by using the five ellipse parameters of the point mark, we may obtain the reconstructed coded target (Fig. 6):

$$
\begin{aligned}
x''_{\mathrm{c}} &= (X_{\mathrm{c}} - X_{\mathrm{o}})\cos\alpha + (Y_{\mathrm{c}} - Y_{\mathrm{o}})\sin\alpha\,, \\
y''_{\mathrm{c}} &= \frac{-a}{b}(X_{\mathrm{c}} - X_{\mathrm{o}})\sin\alpha + \frac{a}{b}(Y_{\mathrm{c}} - Y_{\mathrm{o}})\cos\alpha\,, \\
r &= \sqrt{x''^2_{\mathrm{c}} + y''^2_{\mathrm{c}}}\,, \\
\theta &= \begin{cases} \tan^{-1}(y''_{\mathrm{c}}, x''_{\mathrm{c}})\,, & y''_{\mathrm{c}} \geq 0 \\ \tan^{-1}(y''_{\mathrm{c}}, x''_{\mathrm{c}}) + 2\pi\,, & y''_{\mathrm{c}} < 0\,. \end{cases}
\end{aligned}
\tag{2}
$$

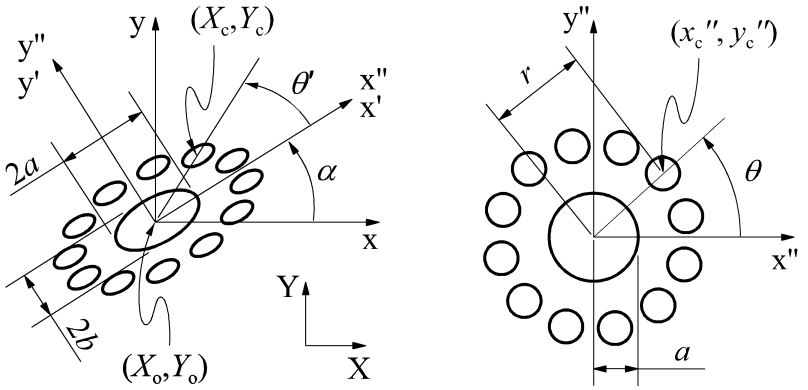

(a) (b)

Fig. 6. Reconstruction of the circular coded target: (a) Definition of the coordinate systems by using the estimated five ellipse parameters (X_o, Y_o, a, b and α) of the point mark; (b) Rearranged coding points around the point mark.

A valid coding point must find itself in a ring shaped zone around the point mark [Fig. 4(c)], and reversibly, a valid point mark must have a valid arrangement of the coding points around it [Figs. 4(d) and 4(e)]. Through certification and interpretation of the arrangement of the coding points, we will get the identification number of the target. A simplified workflow of the image processing for the circular coded target is given in Fig. 7. The resulting image coordinates of the point targets, together with their identification numbers, will be used for the subsequent camera calibration and 3D-point measurement.

For an accurate image point determination of the point mark, and for a reliable rearrangement of the coding points around the point mark [see also Eq. (2)], an accurate estimation of the five ellipse parameters (e.g. ellipse fitting) of the image point mark is inevitable. Here we have applied a *geometric ellipse fitting*,[3] which has the objective function of the orthogonal error distances, and results in an unbiased optimal parameter estimation. Additionally, a *forced orthogonal edge detection* is applied to the contour of the point mark by using the ellipse parameters from a preceding ellipse fitting to the pixel accurate contour points (Fig. 8).[1] As a result, robust and meaningful edge detection is made possible also in a very noised image (e.g. image of the coded targets with a superimposed random pattern).

In this paper, we have applied a three-step procedure to the detection and fitting of the target contour. In the first step, we extract the target contour points from binary image and apply an ellipse fitting to these pixel accurate contour points. In the next step, subpixel accurate contour points will be obtained through forced edge detection in gray image along the orthogonal path to the estimated ellipse (Fig. 8). As a result, the succeeding ellipse fitting will be more reliable and accurate than the preceding one to the pixel accurate contour points. The length constraint on the image interpolation path keeps the edge detection from straying away with

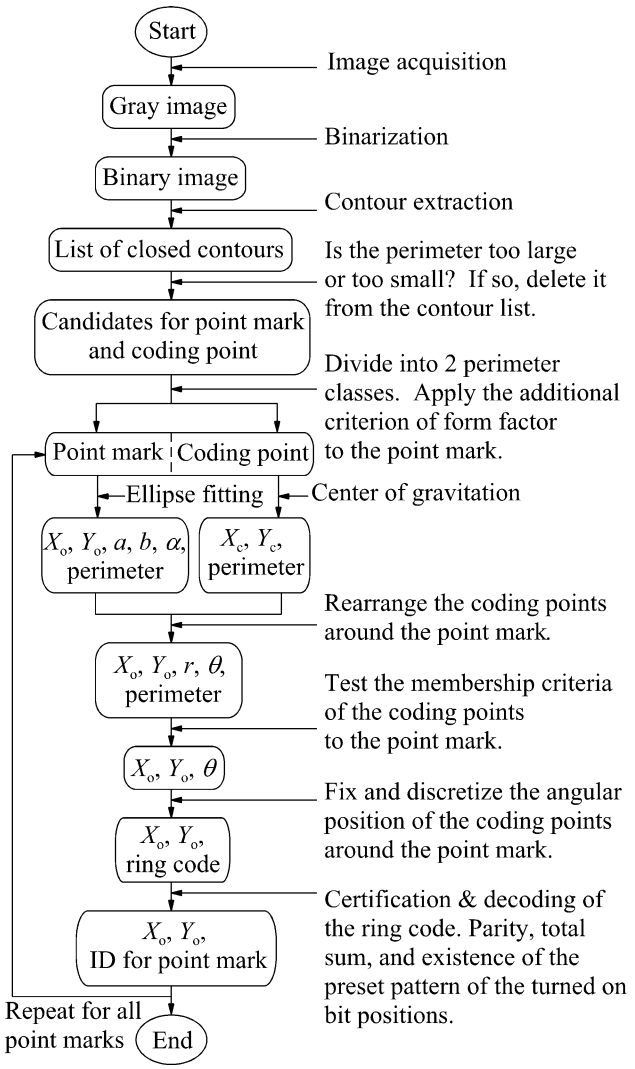

Fig. 7. A simplified work flow of the image processing applied to the image of circular coded targets.

an image of low quality. In the final step, ellipse fitting to these subpixel accurate contour points will be applied where the image gradient information across the boundary of the image ellipse can be used as the weighting values of the individual contour points with ellipse fitting. If the accuracy level demanded by the camera calibration and/or by the 3D-measurement is not high, only the first step with an *algebraic ellipse fitting*[6] to the pixel accurate contour points could be carried out alone. For a high-accuracy measurement project, all three steps, including the geometric ellipse fitting[3] to the subpixel accurate contour points, are recommended.

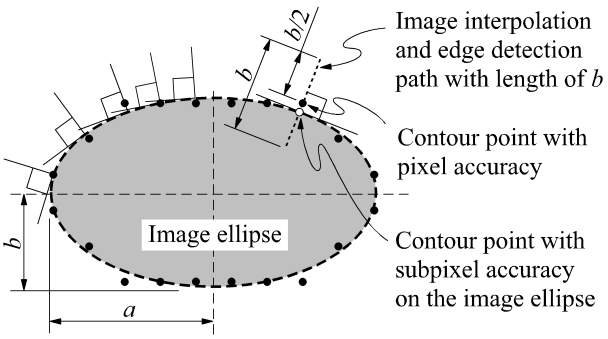

Fig. 8. Forced image interpolation and edge detection along the orthogonal path to the image ellipse.

4. Applications to Optical 3D-Measurement and Camera Calibration

4.1. *Standard optical 3D-measurement with stereo or multiple imaging*

In general, in order to estimate the parameters of a system, some observations must be made by all system components whose parameters are essentially involved in the functionality of the system. Given the system model, the model parameters can be estimated through an analysis of the observations. In the case of stereo, or multi-imaging vision systems, several widely accepted system models (camera model) and system parameter estimation (camera calibration) algorithms are already available. What we have yet to do is determine the homologous image point coordinates for some given object points (Fig. 1). As the simplest application example, this task can be taken over by the circular coded target and its image processing (Fig. 9).

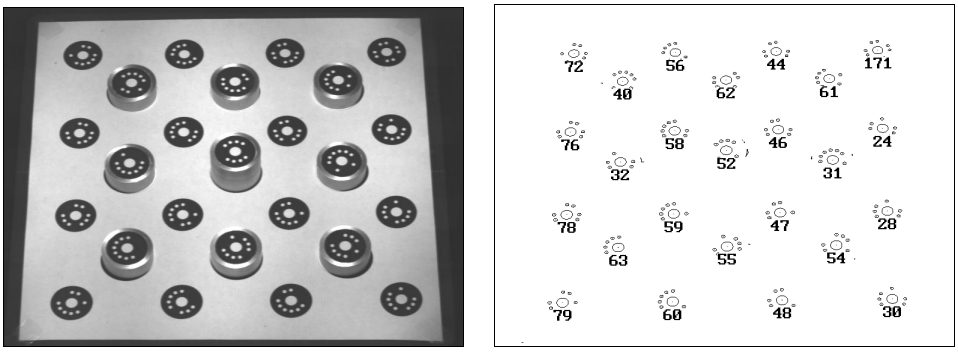

(a) (b)

Fig. 9. Standard application of the circular coded target to 3D-point measurement and camera calibration: (a) Target field with a number of circular coded targets; (b) Positioned and identified targets.

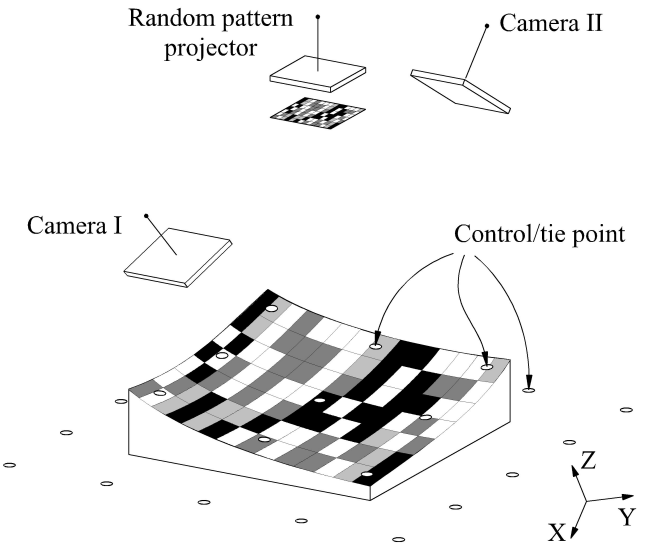

Fig. 10. Setup of the random pattern projecting 3D-measurement method.

4.2. *Random pattern projection method*

A more difficult but very successful industrial application of the circular coded target is the camera calibration for the *random pattern method*.[13,15,18] The hardware setup of the measuring system is comprised of two high-resolution CCD cameras (e.g. Kodak DCS 460 with image format of 3072×2048 pixel) and a random pattern projector (Fig. 10). The projector distinctly marks the object surface, and the two cameras simultaneously capture the patterned object surface, hence providing a stereoscopic view of the scene. For the purpose of the surface point measurement through image correlation and triangulation, the camera parameters at the moment of the stereoscopic imaging of the patterned object surface should be estimated. This means that both the object targets for the camera calibration and the patterned object surface for the image correlation are to be imaged at the same time in each image [Fig. 11(a)]. The camera parameters will be estimated through an analysis of the image coordinates of the coded targets (camera calibration). Then with the known camera parameters, the image correlation of the patterned object surface can be effectively carried out using the epipolar constraints, and we will obtain the two observation rays for each 3D-point on the object surface.

Simultaneous imaging of the targets and patterned object surfaces is the only secure method providing the camera parameters at the moment of the image capturing of the patterned object surface. Of course, we can capture the object surface with coded targets in two separate steps, with and without random pattern projection. However, we cannot always exclude a movement of the camera, and/or of the measurement object, during the two-step image capturing. Furthermore, considering a measurement project with a large number of image capturing, the memory cartridge

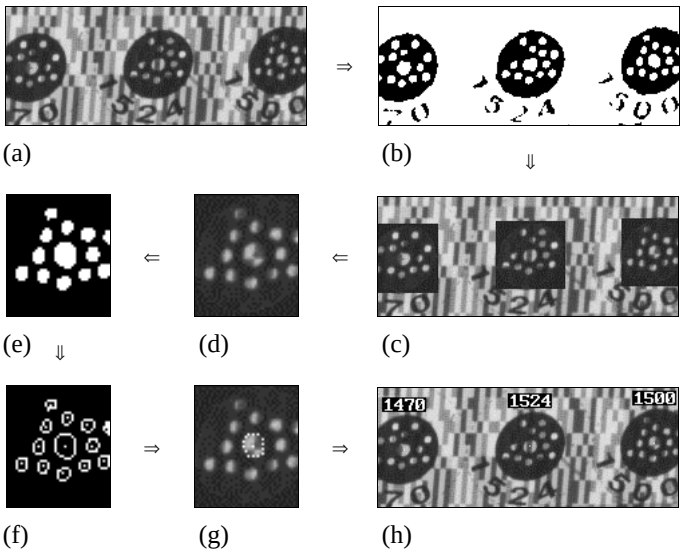

Fig. 11. Image processing of the circular coded target with superimposed random pattern: (a) Gray image (225×90 pixel); (b) Optimal thresholding concerning the size and form factor of the target background plate; (c) Masked image areas for target; (d) Local gray image block; (e) Local thresholding; (f) Contours of the point mark and the coding points; (g) Edge detection, and the estimated center of the point mark; (h) Identified and positioned target center.

of the hand-carried digital camera has only a limited frame capacity. Image capturing should be carried out as quickly as possible, and loading of a new memory cartridge during a measurement project must be prevented in order to not only save the overall measuring costs, but also guarantee the stability of the intrinsic parameters for all captured images. More detailed descriptions of the system construction and the measurement principle are given in Refs. 13, 15 and 18.

We describe in detail the image processing strategy used for detecting the circular coded targets in the image superimposed with the random pattern. The constraints on the target geometry (as described in Secs. 2 and 3) play an important role and guarantee a reliable object detection and identification. First, to locate the target image areas, we have searched for the circular background plates in the binary image [Fig. 11(b)], taking advantage of the size effect of the background plates over the point mark. The optimal binarization for a group of image ellipses could be characterized by the compactness of each image object and by the object detection rate. We have investigated some cumulative compactnesses as the performance indexes for the image binarization:

$$\begin{aligned} C_1 &= \sum_i \frac{1}{F_i}\,, \quad C_3 = \sum_i \frac{1}{F_i - 1}\,, \\ C_2 &= \sum_i \frac{A_i}{F_i}\,, \quad C_4 = \sum_i \frac{A_i}{F_i - 1}\,, \end{aligned} \tag{3}$$

where F_i is the form factor, and A_i is the area of an individual image object. By the binarization of the gray image with some target background plates [Fig. 11(a)], we have plotted in Figs. 12(a) and 12(b) the cumulative compactness as the function of the thresholding values. We have summed up in Eq. (3) only the image objects in the binary image, which satisfy the criteria of size and form factor for the background plate [Fig. 4(a)]. We see that the cumulative compactness of C_3

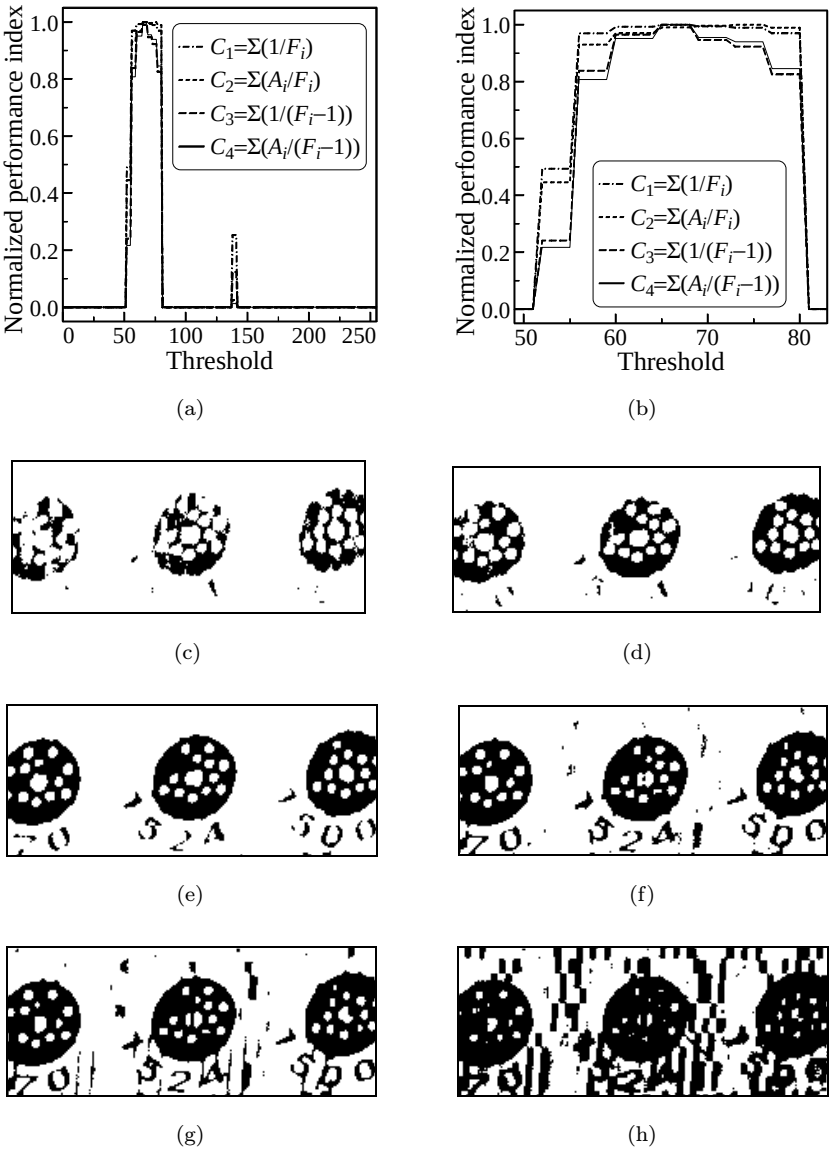

Fig. 12. Optimal binarization for the image of the circular object targets by using the cumulative compactness as the performance index: (a and b) Dependence of the cumulative compactness on the thresholding values; (c) Threshold at 50, (d) 54, (e) 66, (f) 79, (g) 82, (h) 140 respectively.

and C_4 distinguishes the thresholding values very well. C_3 and C_4 increase very fast, as the form of each image object is similar to a circle (i.e. $F_i \approx 1$). The binary images of Figs. 12(c) to 12(h) confirm the validity of C_3 and C_4 as the performance indexes of the binarization with regard to the extraction of the circular targets in an image. The optimal thresholding value (e.g. about 66 for Fig. 11(a)) can be searched by using the coarse-to-fine strategy in combination with the initial starting value provided from a histogram analysis.

Once the image area for a target is localized [Fig. 11(c)], we apply a local image processing to the small image window [Figs. 11(d)–11(g)]. Here, we use the cumulative compactness C_4 for an optimal binarization of the coding points and the point mark. Only the image objects satisfying the object criteria for coding points and point mark are to be summed up in C_4 of Eq. (3) [Figs. 4(a)–4(c)]. If two or more coding points are merged together into a larger one through a low thresholding value, the resulting image object is too large and/or too complex and may not be accepted as a valid coding point, and C_4 will have a smaller value. In comparison to C_3, the weighting through the object area in C_4 forces coding points to be binarized as large as possible. In other words, if a coding point is too small, or removed from the binary image through a high thresholding value, C_4 will again have a smaller value. As a result, we acquire clear and well separated/positioned coding points around the point mark in the binary image [Figs. 11(e) and 11(f)], from which a reliable decoding of the code information will be made possible.

5. Summary

Alongside the accuracy and stability of measurement results, automation of measurement procedures is indispensable for the future industrial application of optical 3D-measurement techniques. In this paper, we have presented a new circular coded target, its image processing and its application to the optical 3D-measurement method. The programmable arrangement of the coding points provides the adaptability of the target for all possible measuring tasks occurring in practice. The special geometric construction of the target, and the proper image processing, make possible an accurate and reliable image point measurement and identification. The outstanding performance of the circular coded target originated from the fact that it is comprised only of circles, i.e. circular point mark, circular coding point, circular background disk, and circular arrangement of the coding point around the point mark. A circle will be projected as an ellipse in the image plane, and an ellipse is a relatively compact image object. From the geometric design to the image processing of the circular coded target, we have utilized all these geometric natures of a circle as concerning to projective imaging. The circular coded target is successfully integrated in a commercial digital photogrammetric system for surface reconstruction with random pattern projection.[15] Furthermore, we expect a wide acceptance of the proposed coded target with industrial applications with regard to accuracy, reliability and the automation of the 3D-measuring task.[16]

References

1. S. J. Ahn, "Kreisförmige Zielmarke (Circular target)," *Proc. 4. ABW Workshop Optische 3D-Formerfassung*, January 22–23, 1997, Technical Academy Esslingen, Germany, 17 pages, URL: http://www.fh-nuertingen.de/∼ag3d/lit/ahn_97.zip, July 10, 2001.
2. S. J. Ahn and B. Oberdorfer, "Optoelektronisch erfaßbares Identifizierungs- oder Zielelement sowie Verfahren zu seiner Erfassung," German Patent, DE 196 32 058 C1, filed: August 9, 1996, issued: March 5, 1998.
3. S. J. Ahn and W. Rauh, "Geometric least squares fitting of circle and ellipse," *Int. J. Pattern Recognition and Artificial Intelligence* **13**, 7 (1999) 987–996.
4. S. J. Ahn and M. Schultes, "A new circular coded target for the automation of photogrammetric 3D-surface measurements," *Proc. 4th Conf. Optical 3-D Measurement Techniques*, September 29–October 2, 1997, Zurich, Switzerland, pp. 225–234.
5. S. J. Ahn, H.-J. Warnecke and R. Kotowski, "Systematic geometric image measurement errors of circular object targets: mathematical formulation and correction," *Photogramm. Record* **16**, 93 (1999) 485–502.
6. F. L. Bookstein, "Fitting conic sections to scattered data," *Comput. Graph. Imag. Process.* **9** (1979) 56–71.
7. C. B. Bose and I. Amir, "Design of fiducials for accurate registration using machine vision," *IEEE Trans. Patt. Anal. Mach. Intell.* **12** (1990) 1196–1200.
8. T. Caesar and M. Michaelis, "Ein neues Verfahren zur robusten Erkennung textcodierter Meßmarken," *Zeitschrift für Photogrammetrie und Fernerkundung* **65** (1997) 150–157.
9. C. S. Fraser, "Automation in digital close-range photogrammetry," *Proc. First Trans Tasman Surveyors Conf.*, April 12–18, 1997, Newcastle, Australia, pp. 8.1–8.10.
10. C. S. Fraser and D. C. Brown, "Industrial photogrammetry: new developments and recent applications," *Photogramm. Record* **12**, 68 (1986) 197–217.
11. A. S. Homainejad and M. R. Shortis, "Development of a template for automatic stereo matching," *Int. Arch. Photogramm. Remote Sensing* **30**, 5W1 (1995) 318–322.
12. M. Knobloch and T. Rosenthal, "MIROS: a new software for Rollei RS1 digital monocomparator," *Int. Arch. Photogramm. Remote Sensing* **29**, B5 (1992) 35–42.
13. P. Krzystek, F. Petran and H. Schewe, "Automatic reconstruction of concept models by using a digital photogrammetric measurement system," *Int. Arch. Photogramm. Remote Sensing* **30**, 5W1 (1995) 176–185.
14. M. Niederöst and H.-G. Maas, "Automatic deformation measurement with a digital still video camera," *Proc. 4th Conf. Optical 3-D Measurement Techniques*, September 29–October 2, 1997, Zurich, Switzerland, pp. 266–271.
15. N. N., "MATCH-I: automatic 3D digitisation of industrial surfaces using digital cameras and image matching techniques," URL: http://www.inpho.de/match_i.htm, July 10, 2001.
16. N. N., "CIRCO: circular coded target," URL: http://www.inpho.de/coded.htm, July 10, 2001.
17. F. A. Russo and R. P. Knockeart, "Automated data acquisition with an optical code reader," *Bendix Techn. J.* **5** (1972) 48–52.
18. H. Schewe, "Automatische photogrammetrische Karosserie-Vermessung," *Bildmessung und Luftbildwesen* **56** (1988) 16–24.
19. C.-T. Schneider, "3-D Vermessung von Oberflächen und Bauteilen durch Photogrammetrie und Bildverarbeitung," *Proc. IDENT/VISION '91*, May 14–17, 1991, Stuttgart, Germany, pp. 90–93.

20. G. Trenkler, "Anordnung zur automatischen Sortierung von Stückgütern, insbesondere quaderähnlicher Form," German Patent, DE 30 10 112 A1, filed: March 15, 1980, laid open: September 24, 1981.
21. F. A. van den Heuvel, R. J. G. A. Kroon and R. S. Le Poole, "Digital close range photogrammetry using artificial targets," *Int. Arch. Photogramm. Remote Sensing* **29**, B5 (1992) 222–229.
22. K. W. Wong, M. Lew and G. Wiley, "3-D metric vision for engineering construction," *Int. Arch. Photogramm. Remote Sensing* **27**, B5 (1988) 647–656.

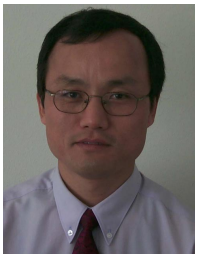

Sung Joon Ahn graduated with B.S. degree in mechanical design and production engineering from the Seoul National University in South Korea in 1985. He obtained his M.Sc. degree in production engineering from the Korea Advanced Institute of Science and Technology (KAIST) in 1987. He worked as a junior research scientist at the Research Center of LG Electronics, Ltd. in Seoul from 1987 to 1990. Since 1991, he has been working as a research scientist for the Fraunhofer Institute for Manufacturing Engineering and Automation (IPA) in Stuttgart, Germany.

His research interests include pattern recognition, optical 3D-measurement, and camera calibration.

Sung Il Kim received his M.Sc. degree in biomechanics from the Korea University, Seoul, South Korea, in 1993. From 1993 to 1996 he worked as a teaching professor of physical education in the Republic of Korea Air Force Academy. He is currently a Ph.D. candidate in biomechanics, physical education at the Korea University.

His current research interests are motion analysis, target detection, and optical 3D-measurement.

Wolfgang Rauh received his Doctorate in 1993 from the University of Stuttgart. He worked at the University of Stuttgart from 1984 until 1989 after having received his Diploma in Mechanical Engineering from the University of Karlsruhe in 1984. He then became head of the group "Industrial Image Processing" at the Fraunhofer Institute for Manufacturing Engineering and Automation (IPA). In 1991, he was made head of the "Information Processing" department at the same institute. In this department, a wide variety of projects in the area of image processing are carried out.